Bilayer Growth in a Metallic System: Au on Ag(110)

P. Fenter and T. Gustafsson

Department of Physics and Astronomy and Laboratory for Surface Modification, P.O. Box 849, Rutgers—The State University of New Jersey, Piscataway, New Jersey 08854

(Received 17 November 1989)

We report the first observation of a novel growth mode in a metal on metal epitaxy system: *bilayer* formation in Au overlayers grown on Ag(110). By using medium-energy ion scattering to determine the morphology and structure of the overlayers, we find direct evidence that bilayers form spontaneously over a wide range of coverages. We discuss the possible causes of this unusual growth behavior.

PACS numbers: 68.55.Jk, 61.16.Fk, 61.50.Cj, 68.35.Bs

The Au-on-Ag system is an interesting model system in the study of epitaxial growth. The difference in lattice parameter between the two metals is unusually small (4.08 vs 4.09 Å), and the surface free energy of Au ($\gamma_{Au}=1.6$ J/m^2) is only slightly larger than that of Ag ($\gamma_{Ag}=1.3$ J/m^2).[1] Therefore, the Au-on-Ag system is expected to follow an ideal layer-by-layer [i.e.,. a Frank-van der Merwe (FW)] growth mode.[2] This has been clearly shown by Feldman and collaborators several years ago in the case of Au on Ag(111),[3] and less direct evidence exists for the case of Au on Ag(100).[4] In this Letter, we will describe results of an experimental study using medium-energy ion scattering on the growth of Au on Ag(110). These data show unambiguously that the initial growth of Au on this surface is very different from the other two low index surfaces in that it occurs via island formation in *bilayers*. In addition, we find that these bilayer units grow in 3D clusters [that is, in a Volmer-Weber (VW) growth mode] when the surface is more than half covered. As far as we know, this is the first example of bilayer growth in a metallic system.

The strength of ion scattering as a structural probe is that it is quantitative (that is, the scattering cross section is well known in the energy range in which we work). The basic quantity measured in our experiment is the number of backscattered ions (in absolute units) as a function of energy and scattering angle (ϑ_s). This can be directly converted to the number of visible target atoms. Ion scattering is ideally suited to study the growth of Au on Ag because the large mass difference allows the Au and Ag signals to be resolved. This allows us to independently probe the structure of the substrate and the overlayer as a function of overlayer coverage (Θ).

A central concept in the analysis of our data is *shadowing*.[5] An ion beam incident in a random direction will be scattered equally by all atoms within its penetration depth, and therefore the total atomic density is measured. If the beam is incident along a row of atoms (channeling), only the first atom in the row will be completely visible to the incident beam, while atoms in deeper layers will be less visible due to *shadowing*. Ions that are scattered by subsurface layers and attempt to exit along a crystallographic direction will be scattered out of these directions (*blocked*) resulting in lower yields. The position and depth of the "blocking dips" provide direct structural and morphological information.

The Ag(110) crystal was prepared and cleaned using standard surface-science procedures.[6] It was characterized with low-energy electron diffraction [exhibiting a well defined (1×1) pattern], and Auger spectroscopy using a double-pass cylindrical-mirror analyzer (showing no detectable impurities). The incident protons were accelerated with a very stable 400-keV ion accelerator[7] and the backscattered signal (number of ions versus angle) was measured with a high-resolution toroidal energy analyzer.[7] The Au films were grown at room temperature by evaporation from a W filament at a rate of roughly 1 monolayer (ML)/min (1.0 ML$=8.45\times10^{14}$ atoms/cm^2). The Au films exhibit a (1×1) symmetry for all coverages reported here, unlike the Au(110) surface which has a (1×2) missing-row reconstruction.[8] The coverages quoted below were obtained directly from the ion-beam signal and put on an absolute scale by comparison with a calibrated standard.[5]

We first demonstrate that the Au atoms occupy positions close to Ag lattice sites, i.e., *that the growth is epitaxial*. Figure 1 shows the dependence of the number of visible substrate Ag atoms (yield) upon the Au coverage. Initially, the Ag yield exhibits a linear decrease with Au coverage. The decrease is due to Au atoms which shadow Ag atoms; that is, Au grows epitaxially.[3] We also show a plot of χ_{min} for Au as a function of Ag coverage. χ_{min} is the ratio of the visible Au yield in channeling to that in nonchanneling, and is therefore a direct measure of Au-Au shadowing.[3] Below $\Theta_c\approx1$ ML, $\chi_{min}=1.0$, which is consistent with all Au atoms arriving at the surface shadowing only Ag atoms and not Au atoms. Because of the openness of the Ag(110) surface, there are 2 ML of Ag visible to the ion beam [see Fig. 2(a)]. Therefore, χ_{min} can be less than 1.0 only when sites in the third-layer Au are occupied. If Au were growing in a FM mode, there should be no reduction in χ_{min} (i.e., no Au-Au shadowing) for coverages below 2.0 ML, at

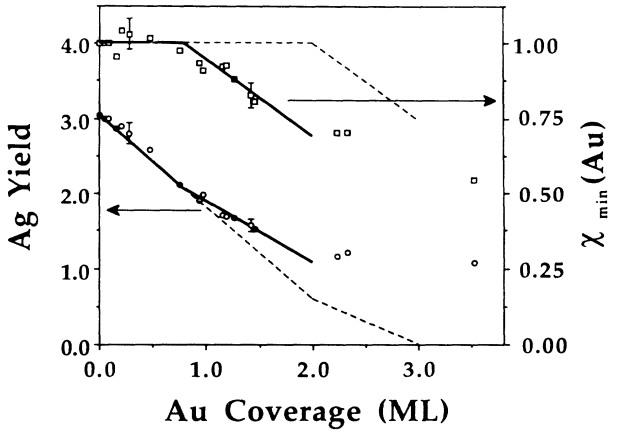

FIG. 1. Single alignment Ag yield in ML (circles) and Au χ_{min} (squares) plotted vs Au coverage for a 100-keV proton beam incident along $[\bar{1}\bar{1}0]$ and detected in the $(\bar{1}11)$ scattering plane at $\vartheta_s = 130°$. The solid and dashed lines are guides to the eye and show what is expected for both the bilayer model (described in the text) and FM growth, respectively. The break observed near 1 ML is due to third-layer occupancy of Au atoms. Note that if the Au were to grow in a "bilayer-by-bilayer" fashion, it would be indistinguishable from FM growth in this type of plot.

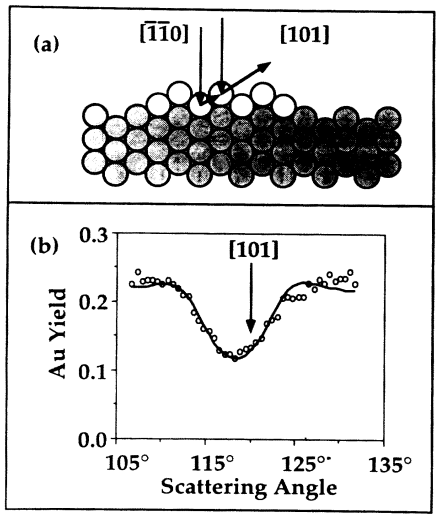

FIG. 2. (a) Side view of the crystal in the $(\bar{1}11)$ plane. Open (shaded) circles indicate Au (Ag) atoms. Arrows indicate the incident $[\bar{1}\bar{1}0]$ ion direction. Note that one-half of the ions are blocked in the [101] blocking direction. (b) Au yield (ML) as a function of scattering angle for the geometry in (a). Circles are data points and the solid line is a Monte Carlo simulation for bilayer growth, assuming bulklike vibrational amplitudes for the Au atoms. Note the deep blocking dip. (The shift in the blocking direction away from [101] is the result of the change in the lattice spacing from the bulk value.) The ion energy was 100 keV.

which point the Ag yield should be greatly reduced. This is clearly not the case, ruling out a FM growth mode. In addition, the linear reduction in the Ag yield implies that there is no disruption of the Ag substrate, and therefore no surface alloying or intermixing taking place.

In order to understand the structure of the Au layers below 1 ML we have taken channeling and blocking data in the $(\bar{1}11)$ scattering zone (Fig. 2). The Au coverage is essentially the same in channeling (0.22 ML) and random incidence (0.23 ML), which rules out any Au-Au shadowing. The data are characterized by a deep blocking dip at $\vartheta_s = 118°$ near the [101] blocking direction. This dip is due to ions which scatter off Au atoms and then are blocked by other Au atoms upon exiting from the crystal so that they cannot reach the detector in this direction. The yield at the blocking-dip minimum is very close to *one-half* of the yield in the shoulders. This implies directly that one-half of the Au atoms occupy *second*-layer sites.

Further support for this model comes from the data in Fig. 3, obtained in the $(\bar{1}10)$ scattering zone. Blocking in this scattering zone probes alternate rather than consecutive layers [Fig. 3(a)]. In this geometry, the [114], [116], and [118] blocking directions should be visible if third-layer sites were occupied.[8] The data in this zone are completely featureless. This implies that there is no significant third-layer occupancy at this coverage.

Aside from trivial scaling factors, exactly the same results as in Figs. 2 and 3 are obtained from the very smallest coverages studied (0.06 ML) up to near 1 ML. We conclude that in this coverage range, Au grows epitaxially on Ag(110) in a *bilayer* form. For this to be possible the mobility of the Au atoms on the surface has to be quite high, but this is known to be the case.[3,9] As 1 ML is the coverage corresponding to one Au atom per Ag (1×1) unit cell, at this coverage only one-half of the surface is covered with Au bilayers (presumably in islands). We can estimate the domain size of the bilayers by considering that there should always be one fewer Au atom in the top layer than in the bottom one [as shown in Fig. 2(a)]. A finite island size would then reduce the depth of the blocking dip due to edge effects. We find a very rough estimate of the island size as 40 Å, above which edge effects become small. Since we see no coverage dependence of the surface blocking-dip depth, this implies that the island size is most likely larger than this even for the smallest Au coverage (0.06 ML).

It is now possible to understand the growth mode of the Au overlayers based upon the data in Fig. 1. At coverages above 1 ML, χ_{min} decreases, directly implying that third- (or higher-) layer sites are being occupied. (Since we have already shown that Au is growing in bilayers, the break could occur at any coverage below 2 ML.) Therefore, Au is growing in a bilayer VW growth mode (three-dimensional islanding before covering the substrate). The information from the blocking curves was essential in reaching this conclusion; from the data in Fig. 1 only, one might simply assume that the Au had

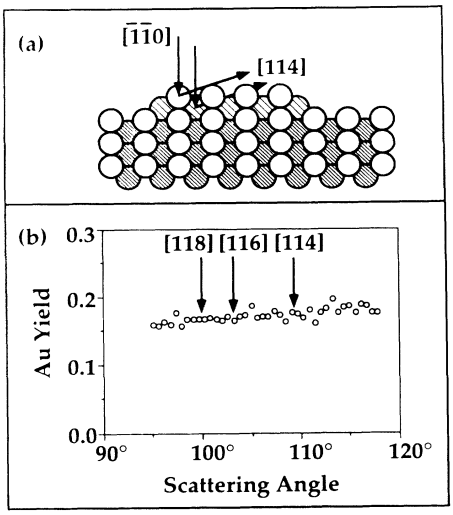

FIG. 3. (a) Side view of the crystal in the ($\bar{1}$10) scattering plane. Light (dark) circles are Au (Ag) atoms, and cross hatching indicates atoms which are in a second independent scattering plane. Arrows indicate the incident [$\bar{1}\bar{1}$0] direction and the [114] blocking direction. (b) Au yield (ML) in this plane. Positions of the [114], [116], and [118] blocking directions are noted. The ion energy was 200 keV.

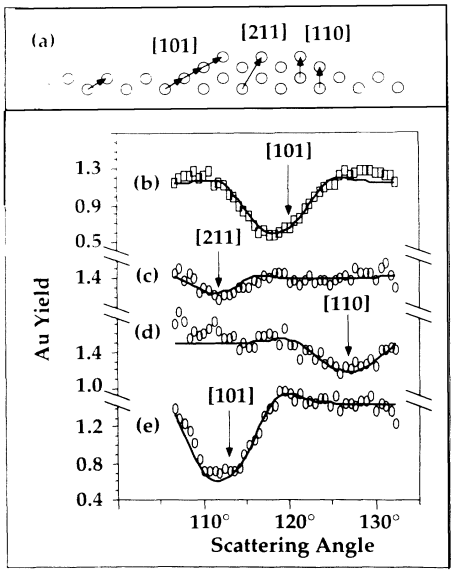

FIG. 4. (a) A schematic picture of the morphology of 1.4 ML Au (substrate not shown). The characteristic blocking directions ([211], [110], and [101]) are indicated. (b)–(e) Planar channeling data of Au yield (ML) taken in the ($\bar{1}$11) plane at incident-ion-beam directions of (b) $\vartheta_i = 0°$, (c) 38°, (d) 53°, and (e) 7° (with respect to the surface normal). The blocking directions are indicated. The circles are data and the solid lines are simulations for perfect bilayer growth. The ion energy was 100 keV.

completed the first monolayer and continued to grow in 3D clusters above Θ_c (i.e., a Stranski-Krastanov mode).

To understand the morphology of the Au overlayer in detail at coverages above 1 ML, we have taken data at a series of incident angles, corresponding to channeling and blocking (as before), *as well as planar channeling and blocking.* In planar channeling the incident beam is *not* aligned with a channeling direction, so that now all atoms in the Au overlayer are visible to the beam (but ions may still be blocked upon exiting). By monitoring the backscattered yield at different incident angles, one can get direct information about the occupancy (if any) of the second, third, fourth, etc., layers, because occupancy in each of these layers results in a characteristic blocking direction. Specifically, blocking along the [101], [110], and [211] directions is due to second-, third-, and fourth-layer occupancies, respectively [Fig. 4(a)].

In Fig. 4(b), we show channeling and blocking data (near the [101] blocking direction) at a total Au coverage of 1.41 ML. In channeling, only 1.2 ML of Au are observed. This directly implies Au-Au shadowing, and, in particular, it provides a lower limit of 0.2 ML for the coverage of third and higher layers.

Figure 4(c) shows the angular dependence of the planar channeling and blocking yield near 112°, which corresponds to the [211] blocking direction. Since this blocking direction corresponds to first-to-fourth-layer blocking, the presence of this dip directly shows that now sites in the fourth layer are occupied. The reduction of the Au yield at the dip (~0.15 ML) is a measure of this occupancy [Fig. 4(a)]. Further, the magnitude of the dip around the [110] direction (and hence the combined third- and fourth-layer coverage) is ~0.3 ML and therefore, the third-layer coverage is also ~0.15 ML [Fig. 4(d)]. Finally [Fig. 4(e)], the depth of the [101] dip is roughly 0.8 ML, which after subtracting out 0.3 ML due to second-to-third and third-to-fourth-layer blocking gives ~0.5 ML in the second layer.

To proceed further, one has to perform a numerical analysis of the data, using Monte Carlo simulations, which takes into account the details of the scattering events in the different blocking geometries. If we model the data using only bilayers, this leads to a best fit with first-to-fourth-layer coverages Θ_i of $\Theta_{1,2}=0.56$ and $\Theta_{3,4}=0.145$, with a total coverage of 1.41 ML. The agreement with the data is clearly satisfactory (Fig. 4). Lastly, to determine the uniqueness of this simple model, we have allowed Θ_3 and Θ_4 to vary independently, while keeping $\Theta_1=\Theta_2$. Since this will necessarily introduce a new parameter, we have restricted the search to a total coverage of 1.41 ML. Our data are most consistent with $\Theta_{1,2}=0.55$, $\Theta_3=0.18$, and $\Theta_4=0.13$, demonstrating a strong bias for a second bilayer. The data then give a direct and consistent picture of the morphology of the Au layer that clearly leads to the conclusion of *bilayer growth,* not just in the first two layers, but *also subsequently.*

To understand these results it is necessary to explain both the growth mode and the bilayer formation. The VW mode is expected if $\gamma_{Au} > \gamma_{Ag} - \gamma_{int}$, where γ_{int} is the interface free energy.[2] Although γ_{Au} is slightly greater than γ_{Ag}, γ_{int} is expected to be small and negative.[2] (This is supported by the small but negative heat of mixing of Au-Ag alloys, which is negligible at room temperature.[10]) Therefore, this criterion is inconclusive. Since the growth of Au on Ag(111) is very clearly FM,[3] the different growth modes on the (111) and (110) surfaces should be due to microscopic factors.

Since second-layer Au atoms in a bilayer bond mostly to other Au atoms while Au atoms in a single layer bond mostly to Ag atoms, if a simple pair potential is used to explain the preference of bilayers over single-layer growth, initial 3D clustering would be predicted over bilayers. If layer-dependent surface energies are invoked to explain the bilayers, it would require large oscillatory changes to explain the uniformity of the bilayers at submonolayer coverages and the continued growth of the second bilayer. It is known that steps provide nucleation sites for Au atoms.[11] If bilayer growth is due to the presence of steps, this would suggest that the bilayers are due to the microscopic step structure; that is, a double-height step would be the preferred nucleation sites. Since we believe that the bilayer domains are large, the step density on the surface is relatively low. We therefore think that the most likely explanation for bilayer growth involves the open geometry of the Ag(110) surface.

In conclusion, we have found that Au grows epitaxially on Ag(110), and that, for the first few monolayers, the Au films do not show any evidence of the (1×2) reconstruction which is present on the semi-infinite Au(110) crystal surface. In addition, our data demonstrate that Au prefers to grow in a bilayer VW growth mode on Ag(110) over a wide range of coverages. This novel growth mode is not predicted by simple energetic considerations.

We would like to thank M. Chester for his help and many valuable discussions, Dr. D. M. Zehner for lending us the Ag(110) substrate, and Dr. L. C. Feldman and Dr. Y. Kuk for sharing unpublished data. This research was supported by NSF Grant No. DMR-8703897.

[1]L. Z. Mezey and J. Giber, Jpn. J. Appl. Phys. **21**, 1569 (1982).

[2]E. Bauer, Appl. Surf. Sci. **11**, 479 (1982).

[3]R. J. Culbertson, L. C. Feldman, P. J. Silverman, and H. Boehm, Phys. Rev. Lett. **47**, 657 (1981).

[4]T. C. Hsieh, A. P. Shapiro, and T.-C. Chiang, Phys. Rev. B **31**, 2541 (1985).

[5]J. F. van der Veen, Surf. Sci. Rep. **5**, 199 (1985).

[6]E. Holub-Krappe, K. Horn, J. W. M. Frenken, R. L. Krans, and J. F. van der Veen, Surf. Sci. **188**, 335 (1987).

[7]High Voltage Engineering Europa, The Netherlands.

[8]M. Copel and T. Gustafsson, Phys. Rev. Lett. **57**, 723 (1986).

[9]R. C. Jaklevic and L. Elie, Phys. Rev. Lett. **60**, 120 (1988).

[10]*Metals Reference Book,* edited by C. J. Smithells (Plenum, New York, 1967), Vol. 1, p. 232.

[11]M. Klau, in *Elektronen-Mikroskopie in der Feskörperphysik,* edited by H. Bethge and J. Heydenrecih (VEB Deutscher Verlag, Berlin, 1982), p. 429.

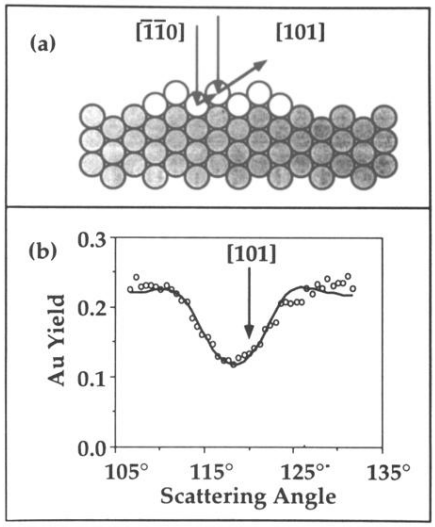

FIG. 2. (a) Side view of the crystal in the $(\bar{1}11)$ plane. Open (shaded) circles indicate Au (Ag) atoms. Arrows indicate the incident $[\bar{1}\bar{1}0]$ ion direction. Note that one-half of the ions are blocked in the [101] blocking direction. (b) Au yield (ML) as a function of scattering angle for the geometry in (a). Circles are data points and the solid line is a Monte Carlo simulation for bilayer growth, assuming bulklike vibrational amplitudes for the Au atoms. Note the deep blocking dip. (The shift in the blocking direction away from [101] is the result of the change in the lattice spacing from the bulk value.) The ion energy was 100 keV.